Eur. Phys. J. D (2016) 70: 138
DOI: 10.1140/epjd/e2016-70239-9

THE EUROPEAN PHYSICAL JOURNAL D

Regular Article

Electronic state spectroscopy by high-resolution vacuum ultraviolet photoabsorption, He(I) photoelectron spectroscopy and ab initio calculations of ethyl acetate*

Malgorzata A. Śmialek[1,2,a], Marta Łabuda[3], Julien Guthmuller[3], Marie-Jeanne Hubin-Franskin[4], Jacques Delwiche[4], Søren Vrønning Hoffmann[5], Nykola C. Jones[5], Nigel J. Mason[2], and Paulo Limão-Vieira[6]

[1] Department of Control and Power Engineering, Faculty of Ocean Engineering and Ship Technology, Gdańsk University of Technology, Gabriela Narutowicza 11/12, 80-233 Gdańsk, Poland
[2] Department of Physical Sciences, The Open University, Walton Hall, Milton Keynes MK7 6AA, UK
[3] Department of Theoretical Physics and Quantum Information, Faculty of Applied Physics and Mathematics, Gdańsk University of Technology, Gabriela Narutowicza 11/12, 80-233 Gdańsk, Poland
[4] Département de Chimie, Université de Liège, Institut de Chimie, Bât. B6C, 4000 Liège, Belgium
[5] ISA, Department of Physics and Astronomy, Aarhus University, Ny Munkegade, Building 1520, 8000 Aarhus C, Denmark
[6] Laboratório de Colisões Atómicas e Moleculares, CEFITEC, Departamento de Física, Faculdade de Ciências e Tecnologia, Universidade NOVA de Lisboa, 2829-516 Caparica, Portugal

Received 5 April 2016/Received in final form 4 May 2016
Published online 16 June 2016

Abstract. The high-resolution vacuum ultraviolet photoabsorption spectrum of ethyl acetate, $C_4H_8O_2$, is presented over the energy range 4.5−10.7 eV (275.5−116.0 nm). Valence and Rydberg transitions and their associated vibronic series observed in the photoabsorption spectrum, have been assigned in accordance with new ab initio calculations of the vertical excitation energies and oscillator strengths. Also, the photoabsorption cross sections have been used to calculate the photolysis lifetime of this ester in the upper stratosphere (20−50 km). Calculations have also been carried out to determine the ionisation energies and fine structure of the lowest ionic state of ethyl acetate and are compared with a newly recorded photoelectron spectrum (from 9.5 to 16.7 eV). Vibrational structure is observed in the first photoelectron band of this molecule for the first time.

1 Introduction

The atmospheric degradation of commonly used volatile organic compounds (VOC) has been of great interest due to their contribution to the green-house effect and acid-rain chemistry. Many such compounds are also known to be formed in the atmosphere due to radical reactions with other compounds that are being released into the atmosphere due to industrial activity, thus it is important to learn more about their chemistry through investigations of the electronic structure of such chemicals.

Esters are one of the most important classes of oxygenated VOCs that are both of industrial and astrochemical interest. Their prominent biogenic source is through their appearance in some fruits, nonetheless, the main source of release to the atmosphere is due to industrial activities. They are mainly used as solvents, fumigants, flavouring and scenting agents. They can also be produced in the troposphere due to hydroxyl radical attack on ethers. It has also been shown that small esters are present in the interstellar space [1].

The significance of ethyl acetate is in its wide use in industry as a solvent, as well as in production of printing ink, glue or paint [2]. Its presence was also detected in the atmosphere of forests in Central Europe due to biogenic sources emissions [3].

Here we report a high resolution VUV photoabsorption spectrum with absolute cross sections of ethyl acetate measured for the first time, accompanied by a photoelectron spectrum (PES) and ab initio calculations on the vertical excitation energies and oscillator strengths of the electronic transitions. Measurement and analysis of the photoelectron spectrum aided the assignment of possible Rydberg transitions in the VUV photoabsorption

* Contribution to the Topical Issue "Low-Energy Interactions related to Atmospheric and Extreme Conditions", edited by S. Ptasinska, M. Smialek-Telega, A. Milosavljevic, B. Sivaraman.

[a] e-mail: smialek@pg.gda.pl

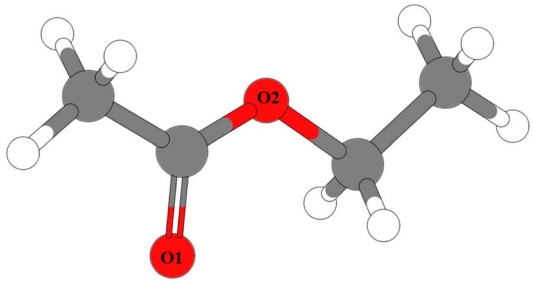

Fig. 1. Structure and numbering of oxygen atoms of the most stable conformer (C_S symmetry) of ethyl acetate; oxygen atoms in red, carbon in grey and hydrogen in white colour.

spectrum. Moreover, for the first time it was possible to resolve and assign vibronic structure in the first ionic band. The only available studies of this molecule concern its first ionisation energy that was obtained either through electron impact mass spectrometry [4–6] or conventional photoelectron measurements [7–9] and PIPECO spectroscopy [10]. The absolute photoabsorption cross sections of ethyl acetate presented here are needed for modeling studies of the Earth's atmosphere and radiation-induced chemistry of esters, and, together with the results on previously analysed members of this class: methyl formate [11], ethyl formate [12] and isobutyl formate [13], will help to understand the chemistry of esters and their electronic state spectroscopies.

2 Structure of ethyl acetate

Among all the possible conformers, *trans-trans* and *trans-gauche* are reported to be the most abundant for the ethyl acetate molecule, with the *trans-trans* being the most stable at room temperature [14]. In the most stable form in the gas phase, ethyl acetate, $C_4H_8O_2$, has C_s symmetry (Fig. 1). In our previous studies on the related compounds of ethyl formate [12] and isobutyl formate [13] it was shown that a proper assignment of the spectroscopic features is obtained using calculations on a single conformer. Therefore, in the present study theoretical computations are only performed on the *trans-trans* conformer. According to our calculations, the electron configuration of the $\tilde{X}^1A'$ ground state is as follows: (a) core orbitals $(1a')^2$ $(2a')^2$ $(3a')^2$ $(4a')^2$ $(5a')^2$ $(6a')^2$, (b) valence orbitals $(7a')^2$ $(8a')^2$ $(9a')^2$ $(10a')^2$ $(11a')^2$ $(12a')^2$ $(13a')^2$ $(1a'')^2$ $(14a')^2$ $(2a'')^2$ $(15a')^2$ $(16a')^2$ $(3a'')^2$ $(17a')^2$ $(18a')^2$ $(4a'')^2$ $(5a'')^2$ $(19a')^2$.

The highest occupied molecular orbital (HOMO, 19a′) in the neutral ground state is localized predominantly on the terminal oxygen in-plane lone pair (n_{O1}). The second highest occupied molecular orbital (HOMO-1, 5a″) shows a main contribution from the oxygen out-of-plane lone pair (n_{O2}). The orbital 4a″ (HOMO-2) corresponds mostly to the bonding π(C=O). The lowest unoccupied molecular orbital (LUMO) is mainly of π^* antibonding character and it is localized on the C=O bond.

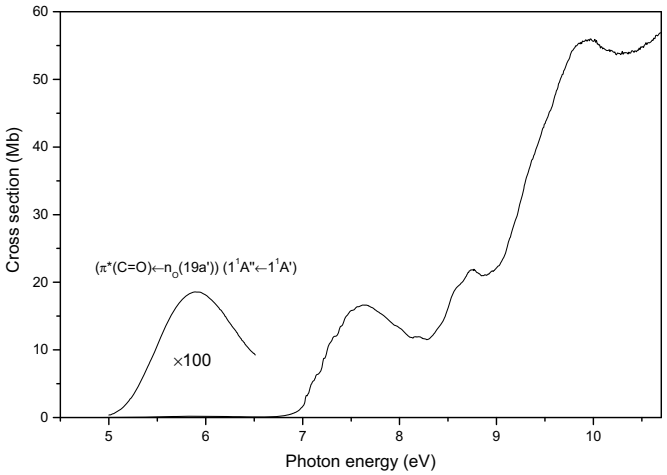

Fig. 2. High resolution photoabsorption spectrum of ethyl acetate; close-up shows the first valence transition, LUMO $\pi^* \leftarrow n_O(19a')$, recorded over the 5.0−6.5 eV range.

3 Experimental

3.1 Ethyl acetate sample

The liquid sample used both in the VUV photoabsorption measurements and the PES experiment was purchased from Sigma-Aldrich, with a purity of 99.8%. The sample was degassed by six freeze-pump-thaw cycles, with no further purification of the sample.

3.2 VUV photoabsorption

The high-resolution VUV photoabsorption spectrum of ethyl acetate (Fig. 2) was measured at the UV1 beam line using the ASTRID synchrotron facility at Aarhus University, Denmark. The experimental set up has been described in detail previously [15]. Briefly, monochromatised synchrotron radiation passes through a static gas sample and a photomultiplier is used to measure the transmitted light intensity. The incident wavelength is selected using a toroidal dispersion grating with 2000 lines/mm providing a resolution of ∼0.075 nm. The minimum and maximum wavelengths between which scans are performed, 115−320 nm (10.8−3.9 eV), are determined by the cut-offs of the windows of the gas cell (LiF entrance and MgF_2 exit) and the grating respectively.

The sample pressure is measured using a capacitance manometer (Baratron). In order to ensure that the data were free of any saturation effects [16,17], the cross section was measured at an appropriate pressure in the range 0.03−1.3 mbar, with typical attenuations <40%. In doing so, we avoided both absorption flattening (when the transmitted intensity is very low), and poorly defined (and hence noisy) spectra when the transmitted intensity is high but close to the incident intensity. The synchrotron beam current is monitored throughout the collection of each spectrum and a background scan is recorded for an

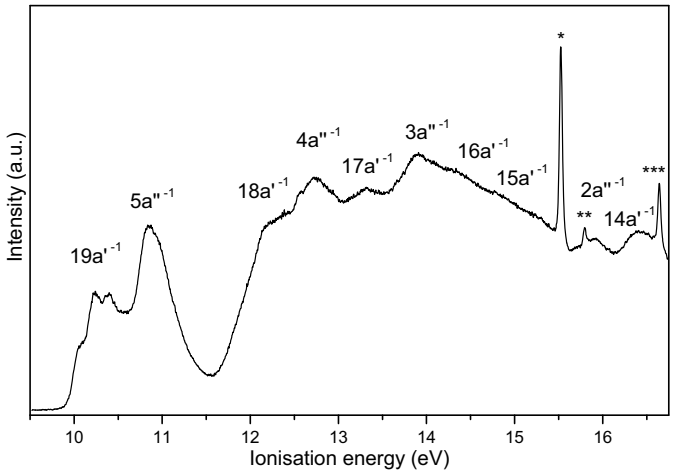

Fig. 3. He(I) photoelectron spectrum of ethyl acetate, $C_4H_8O_2$, in the 9.5−16.7 eV region (*N_2^+ $X^2\Sigma_g^+$, $v' = 0$ produced by the He(I)α line; **N_2^+ $X^2\Sigma_g^+$, $v' = 1$ produced by the He(I)α line; ***N_2^+ $A^2\Pi_u$, $v' = 0$ produced by the He(I)α line).

empty cell. Absolute photoabsorption cross sections are calculated using the Beer-Lambert attenuation law

$$I_t = I_0 \exp(-n\sigma x), \tag{1}$$

where I_t is the radiation intensity transmitted through the gas sample, I_0 is that through the evacuated cell, n is the molecular number density of the sample gas, σ is the absolute photoabsorption cross section, and x is the absorption path length (15.5 cm). The accuracy of the cross section is estimated to be better than ±5%. Only for low values of the absorption ($I_0 \approx I_t$), the uncertainty increases as a percentage of the measured cross section. Specifically, we estimate that the lowest cross section peak of ethyl acetate (about 0.2 Mb near 5.9 eV) to have an uncertainty lower than 15%, which still amounts to only 0.03 Mb.

3.3 Photoelectron spectroscopy

The He(I) (21.22 eV) photoelectron spectrum of ethyl acetate was measured at the Université de Liège, Belgium and is shown in Figure 3. The apparatus has also been described previously in detail [18]. Briefly, it consists of a 180° hemispherical electrostatic analyser with a mean radius of 5 cm. The analyser is used in the constant pass energy mode. The incident photons are produced by a d.c. discharge in a two-stage differentially pumped lamp. The energy scale is calibrated using the $X^2\Sigma_g^+$, $\nu' = 0$ and $A^2\Pi_u$, $\nu' = 0$ peaks of N_2^+, rounded to three decimal places [19,20]. The resolution of the present spectrum is 55 meV and the accuracy of the energy scale is estimated to be ±2 meV. The photoelectron spectrum presented in this paper is the sum of 70 individual spectra. This procedure allows obtaining a good signal-to-noise ratio while keeping the pressure in the spectrometer low ($<5 \times 10^{-6}$ mbar), thus minimizing the occurrence of dimers. For analysis purposes, the spectrum was also deconvoluted according to the van Cittert procedure [21], applied to the ratio method [22]. This technique was only applied in order to bring out some features predicted by the calculations that were hidden in the raw data and should be applied with some care, as described previously [23].

4 Computational methods

The ground state geometry, harmonic vibrational frequencies, and normal coordinates of the neutral singlet state (S_0) and ionic doublet state (D_0) of ethyl acetate were obtained with the Gaussian 09 program [43] by means of second-order Møller-Plesset (MP2) calculations in association with the aug-cc-pVTZ basis set. The ionic state was described by open-shell unrestricted calculations. The first ionisation energies (IE) were computed from the energy difference between the neutral and ionic ground states. The vertical IE was calculated at the ground state geometry of the neutral compound and the adiabatic IE was evaluated using the optimized geometries of the neutral and ionic ground states. Additionally, the first and second ionisation energies were calculated with the coupled-cluster singles and doubles (CCSD), and the coupled-cluster singles, doubles and perturbative triples (CCSD(T)) methods, employing the optimized geometries at the MP2/aug-cc-pVTZ level of approximation. Furthermore, the zero point vibrational energy (ZPVE) corrections to the adiabatic IEs was determined from the MP2/aug-cc-pVTZ harmonic vibrational frequencies. This correction was also applied to the values calculated with the CCSD and CCSD(T) methods. Higher IEs were obtained with the Partial Third Order (P3) and Outer Valence Green's Function (OVGF) propagator methods using the aug-cc-pVTZ basis set and the MP2/aug-cc-pVTZ geometry. The Franck-Condon (FC) factors, associated with the first photoelectron band of ethyl acetate, were calculated using recursive relations and include Duschinsky rotation effects [24–27]. These calculations made use of the ground state geometries, harmonic frequencies and normal coordinates calculated with the MP2/aug-cc-pVTZ method for the neutral (S_0 state) and ionic (D_0 state) forms of ethyl acetate. Next, the vertical excitation energies, oscillator strengths and electronic radial spatial extents of ethyl acetate were calculated with the equation of motion coupled cluster method restricted to single and double excitations (EOM-CCSD) using the MP2/aug-cc-pVTZ geometry. To provide a better description of the Rydberg states, a set of diffuse functions $(6s, 6p, 4d)$, taken from Kaufmann et al. [28] and localized on the central oxygen atom (O2), was added to the aug-cc-pVTZ basis set (named aug-cc-pVTZ + R). These calculations were performed using the MOLPRO programme, ver. 2012.1 [29].

5 Results and discussion

5.1 He(I) photoelectron spectrum

The He(I) photoelectron spectrum of ethyl acetate over the energy range 9.5−16.7 eV is shown in Figure 3.

Table 1. Calculated vertical/adiabatic ionisation energies of ethyl acetate (C_S symmetry) at the MP2/aug-cc-pVTZ geometry, compared with experimental values, all in eV. Adiabatic ionisation energies include ZPVE correction of −0.035 eV.

Configuration	Calculated/eV					Experimental/eV
	P3	OVGF	MP2	CCSD	CCSD(T)	
$^2A'$ ($19a'^{-1}$)	10.617	10.810	10.828/10.414	10.331/9.945	10.405/10.047	10.226/9.996
$^2A''$ ($5a''^{-1}$)	11.319	11.418	12.063	11.119	11.170	10.801
$^2A''$ ($4a''^{-1}$)	12.825	12.922	–	–	–	12.725
$^2A'$ ($18a'^{-1}$)	12.806	12.869	–	–	–	12.287
$^2A'$ ($17a'^{-1}$)	13.614	13.623	–	–	–	13.320
$^2A''$ ($3a''^{-1}$)	13.964	14.035	–	–	–	13.904
$^2A'$ ($16a'^{-1}$)	14.261	14.361	–	–	–	14.337
$^2A'$ ($15a'^{-1}$)	14.769	14.813	–	–	–	14.780
$^2A''$ ($2a''^{-1}$)	15.622	15.664	–	–	–	15.913
$^2A'$ ($14a'^{-1}$)	16.331	16.268	–	–	–	16.398
$^2A''$ ($1a''^{-1}$)	16.932	16.947	–	–	–	–
$^2A'$ ($13a'^{-1}$)	16.947	16.937	–	–	–	–

The calculated vertical and adiabatic ionisation energies obtained for the C_S symmetry of ethyl acetate through various calculation methods, as well as determined based on the present experimental spectrum, are shown in Table 1. The lowest vertical (10.226 eV) and adiabatic (9.996 eV) values of IEs obtained from the spectra agree well with the values obtained from CCSD calculations (10.331 and 9.945 eV, respectively). The experimental results are also in a good agreement with the outcome of the calculations with the CCSD(T) method (10.405 and 10.047 eV, respectively). The calculations predict the adiabatic value with a deviation from experiment of about 0.05 eV, which is in agreement with the results obtained previously for ethyl formate [12] and isobutyl formate [13]. The vertical value for this state agrees well with that obtained by Sweigart and Turner [8] (10.39 eV). The adiabatic value of IE is in a good agreement with the one given by Benoit and Harrison [9] (9.90 eV) and comparable to the one given by Watanabe [7] (10.09 ± 0.02), but lower than that reported by Sweigart and Turner [8] (10.24 eV). The values calculated for higher IEs through P3 and OVGF methods also agree well with the values resulting from the experimental measurement, yielding differences not greater than 0.3 eV between calculated and measured values. Similar results were obtained for other ester molecules analysed previously [11–13]. The IE value obtained for the $^2A''(5a''^{-1})$ state, yielding 10.801 eV, is also comparable with that obtained previously, 10.99 eV [8]. It is worth noticing that the order of states 4a″ and 18a′ is inverted in the calculations with respect to the determined electron configuration of the molecule in its ground state.

In Figure 4, a low energy part of the photoelectron spectrum with resolved $19a'^{-1}$ state (top) is compared with the calculated spectrum obtained from the Franck-Condon factors (bottom). Since the calculated spectrum revealed possible vibronic structure, the experimental spectrum has been deconvoluted using Gauss profiles and is shown in the middle part of the Figure 4. The vibrational transitions calculated for ethyl acetate are shown in Table 2, together with corresponding FC factors.

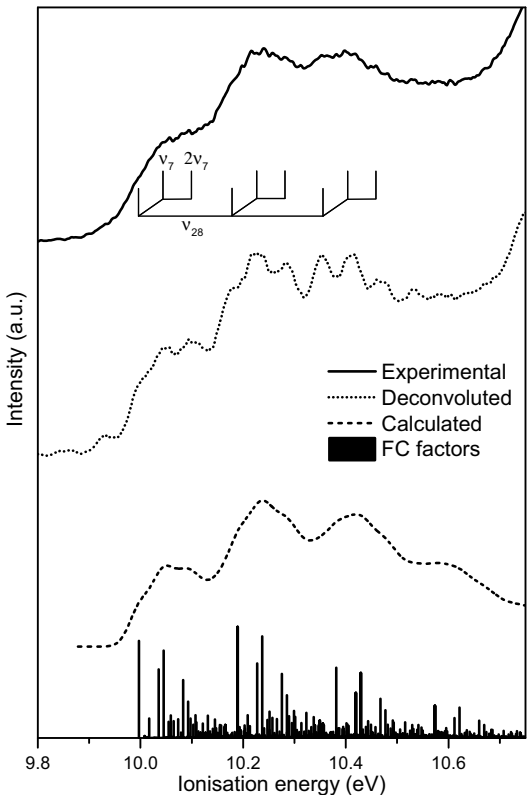

Fig. 4. Comparison between experimental (solid) and theoretical Franck-Condon (dashed) vibrational structure of the first, $^2A'(19a'^{-1})$, photoelectron band of ethyl acetate with vibronic excitation assignment; deconvoluted experimental spectrum (dotted) presents the vibronic structure of the molecule.

From this analysis it was possible to assign the main vibronic structure visible in the $19a'^{-1}$ state to the ν_{28} mode that designates C−O and C=O stretches. This structure is then accompanied by combination bands involving mainly the ν_7 mode that, according to our calculations, corresponds to OCC deformation combined with CO stretch

Table 2. Main vibrational transitions and Franck-Condon (FC) factors contributing to the vibrational structure of the first photoelectron band for ethyl acetate (MP2/aug-cc-pVTZ).

Vibrational state	Frequency[a] (cm^{-1})	FC factor
0-0	0	0.0199
ν_6	308	0.0140
ν_7	386	0.0179
$\nu_6 + \nu_7$	694	0.0119
$2\nu_7$	773	0.0075
ν_{28}	1550	0.0228
$\nu_{28} + \nu_6$	1858	0.0153
$\nu_{28} + \nu_7$	1936	0.0209
$\nu_{28} + \nu_8$	2050	0.0054
$\nu_{28} + \nu_6 + \nu_7$	2244	0.0131
$\nu_{28} + 2\nu_7$	2323	0.0088
$\nu_{28} + \nu_7 + \nu_8$	2437	0.0055
$\nu_{28} + 2\nu_7 + \nu_6$	2631	0.0052
$2\nu_{28}$	3100	0.0144
$\nu_{28} + \nu_{12} + \nu_7$	3148	0.0020
$2\nu_{28} + \nu_6$	3408	0.0093
$2\nu_{28} + \nu_7$	3486	0.0134
$2\nu_{28} + \nu_6 + \nu_7$	3794	0.0080
$2\nu_{28} + 2\nu_7$	3873	0.0057
$3\nu_{28}$	4650	0.0067
$3\nu_{28} + \nu_6$	4958	0.0041
$3\nu_{28} + \nu_7$	5036	0.0062
$3\nu_{28} + \nu_6 + \nu_7$	5344	0.0036

[a] The MP2 vibrational frequencies were corrected by a scaling factor of 0.96 [30].

and CH_3 rocking and can be labelled as the OCC out-of-plane bend [31]. Table 2 and Figure 4 show that mode ν_6 and to a lesser extent mode ν_8 also contribute to the vibronic structure. The energy positions of the vibrational features resolved in the first state in the photoelectron spectrum are presented in Table 3, and are assigned to progressions of modes ν_{28} and ν_7.

5.2 Rydberg series

The photoabsorption spectrum above 6.5 eV shows a number of superimposed structures extending to the lowest ionisation energy. The proposed Rydberg transitions, labeled in Figures 5 and 6 and presented in Tables 4 and 5, originate mainly from the HOMO ($19a'$) according to our calculations. The positions of the peaks, E_n, have been predicted using the well-known Rydberg formula: $E_n = E_i - R/(n-\delta)^2$, where E_i is the ionisation energy, R is the Rydberg constant 13.61 eV, n is the principal quantum number of the Rydberg orbital of energy E_n, and δ is the quantum defect. Quantum defects are expected to be in range of 1.0−0.9, 0.6−0.3 and <0.25 for ns, np and nd series, respectively. The ionisation energy used in this assessment was the vertical value for $19a'^{-1}$, i.e. 10.226 eV.

In the measured experimental spectrum, due to a massive overlap of electronic states that occurs already at low energy, it was not possible to assign the transitions unambiguously, thus the higher members of all series should be treated rather as tentative assignments that were made based on the value of the quantum defect.

Table 3. Energy positions and vibrational analysis of features observed in the first photoelectron band ($19a'^{-1}$) of ethyl acetate.

Peak energy/eV	Assignment	ΔE (ν_7)/eV	ΔE (ν_{28})/eV
9.996	Adiabatic IE	–	–
10.044	$1\nu_7$	0.048	–
10.099	$2\nu_7$	0.055	–
10.178	$1\nu_{28}$	–	0.182
10.226	$1\nu_{28} + 1\nu_7$ (Vertical IE)	0.048	–
10.281	$1\nu_{28} + 2\nu_7$	0.055	–
10.355	$2\nu_{28}$	–	0.177
10.403	$2\nu_{28} + 1\nu_7$	0.048	–
10.458	$2\nu_{28} + 2\nu_7$	0.055	–

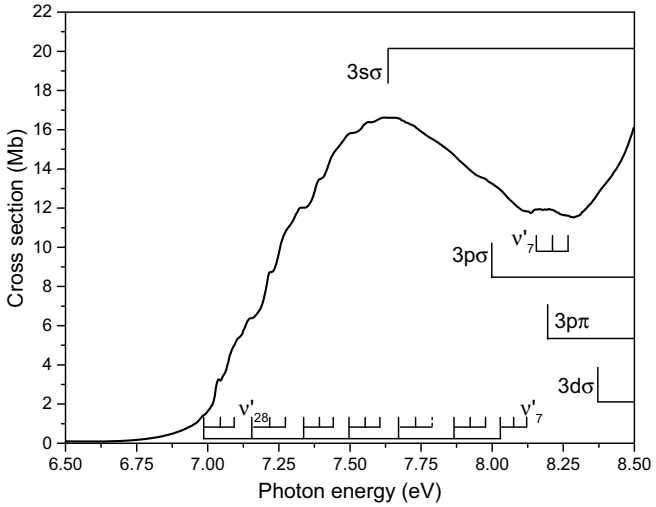

Fig. 5. High resolution photoabsorption spectrum of ethyl acetate over the 6.5−8.5 eV range; dashed line indicates a tentative assignment.

The feature at 7.634 eV was assigned to the ($3s\sigma \leftarrow n_{O1}$, $19a'$) Rydberg transition with a quantum defect of 0.71 (Tab. 4) and is accompanied by fine structure, discussed in Section 5.3. The calculated value of 7.343 eV is in a good agreement with the one found experimentally. The higher members of these Rydberg series are proposed to extend to $n = 4$. State $n = 5$ was assigned purely on the value of the quantum defect.

The first members of $np\sigma$ and $np\pi$ series were found at 8.000 eV and 8.195 eV with quantum defects of 0.53 and 0.41, respectively (Tab. 4). Calculated energies for these transitions (Tab. 5), yielding 8.132 eV and 8.119 eV, agree with experimental values reasonably well, when the possible valence character of these transitions is also accounted for. First members of both np series are also associated with vibronic structure, as shown in Figure 5. The higher members of these Rydberg series were assigned tentatively, based on the value of the quantum defect. The features at 8.372 eV and 8.574 eV were assigned

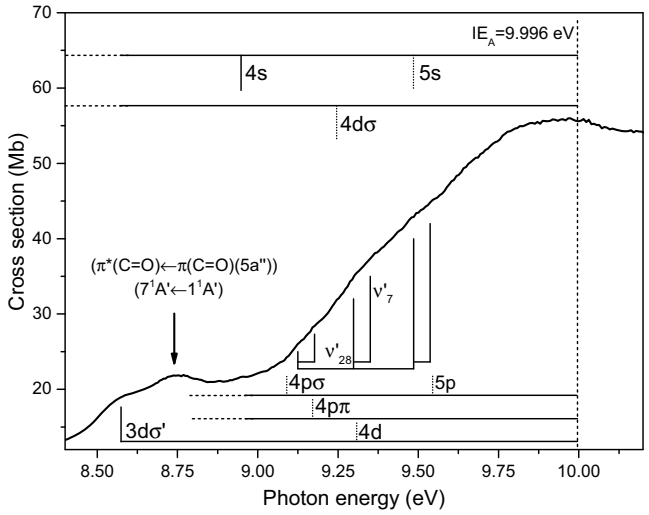

Fig. 6. High resolution photoabsorption spectrum of ethyl acetate over the 8.25−10.75 eV range; dashed line indicates a tentative assignment.

to first transitions of the $nd\sigma$ and $nd\sigma'$, respectively, with corresponding values of quantum defects $\delta = 0.29$ and $\delta = 0.13$. These are also in a sensible agreement with the calculated values of 8.667 eV and 8.856 eV. The higher members of these Rydberg series are difficult to assign due to low values of relative intensities, the overlap with other transitions and vibronic structures and are indicated purely based on the values of quantum defects. It was not possible to distinguish in the spectrum the features that correspond to Rydberg transitions converging to the HOMO-1 (5a″), presumably also due to the low values of their relative intensities as well as their presence in the region of the continuous overlap of other transitions.

5.3 Valence states and transitions of ethyl acetate

Calculated vertical excitation energies of the first thirty states of ethyl acetate, shown in Table 5, allowed assignment of the absorption band centred at 5.904 eV to (π^*(C=O) ← n_{O1}19a′) transition and the one centred at 8.394 eV to the (π^*(C=O) ← n_{O2}5a″) transition (Figs. 2 and 6).

The first band, shown in Figure 2, with a maximum cross section of 0.19 Mb, has been identified as the transition from the terminal oxygen in-plane lone pair (n_{O1}) to the first π antibonding molecular orbital (π^*(C=O) ← n_{O1}19a′)(1^1A″← 1^1A′). The calculated value of the oscillator strength, 1×10^{-3}, is comparable with the values obtained for the previously analysed esters [11–13]. The position of the maximum cross section of this band also agrees well with the value given by others, obtained from the spectrum of the liquid sample, i.e. 5.904 eV [32]. No vibronic structure has been resolved on this band.

It was possible to assign some vibrational progressions in the 6.5−10.0 eV range over the bands identified as pure Rydberg transitions and the details of these assignments are shown in Figures 5 and 6, and are also listed in Table 6.

Table 4. Energies (in eV), quantum defects and assignments of the *ns*, *np* and *nd* Rydberg series converging to the $\tilde{X}^2$A′(19a′$^{-1}$) ionic electronic ground state of ethyl acetate; *t* − a tentative assignment.

Vertical transition energy/eV	Quantum defect, δ	Assignment
7.634	0.71	3sσ
8.950	0.73	4sσ
9.479(*t*)	0.73	5sσ
8.000	0.53	3pσ
9.090(*t*)	0.54	4pσ
9.545(*t*)	0.53	5pσ
8.195	0.41	3pπ
9.171(*t*)	0.41	4pπ
8.372	0.29	3dσ
9.246(*t*)	0.27	4dσ
8.574	0.13	3dσ'
9.308(*t*)	0.15	4dσ'

Pure Rydberg transitions of high oscillator strengths from this region were discussed in Section 5.2 on the Rydberg series.

The most pronounced series over the structure centred at 7.634 eV, from the 3sσ ←19a′ transition, is proposed to be due to the ν'_{28} mode (C−O and C=O stretches) with an average spacing of 0.174 eV, and with two quanta of the ν'_7 mode (OCC deformation combined with CO stretch and CH_3 rocking), spaced on average by 0.054 eV. Another vibration, associated with the (3pπ ←19a′) transition is due to the ν'_7 mode with an average spacing of 0.056 eV.

At 8.394 eV, a (π^*(C=O) ← n_{O1}5a″)(7^1A′←1^1A′) transition was assigned, with a maximum cross section of 13.19 Mb. According to our calculations this is one of the most pronounced features in the spectrum, with a highest value of the oscillator strength of 0.136.

In the higher energy range, where we see a continuous overlap of Rydberg transitions, it was also possible to distinguish two quanta of ν'_{28} mode, spaced by 0.180 eV, each coupled with one quantum of the ν'_7 mode, of on average 0.051 eV.

5.4 Absolute photoabsorption cross sections and atmospheric photolysis

In this work we present the absolute photoabsorption cross sections of ethyl acetate measured for the first time. Since this compound is of environmental importance, due to being widely used as an industrial solvent, it is of interest to use these absolute cross sections in combination with solar actinic flux [33] measurements from the literature to estimate the photolysis rate of ethyl acetate in the atmosphere from an altitude close to the ground to the stratopause at 50 km. Details of the program used to perform the calculations are presented in a previous publication [34]. The quantum yield for dissociation following absorption is assumed to be unity. The reciprocal of the photolysis rate

Table 5. Calculated vertical excitation energies (EOM-CCSD/aug-cc-pVDZ+R) (in eV) and oscillator strengths for the first 30 states of ethyl acetate compared with the present experimental vertical energies and VUV absorption cross sections.

State	E/eV	f_L	$\langle r^2 \rangle$	Main character	E_{exp}/eV	Cross section/Mb
A″	5.957	0.0010	82	19 a′ → LUMO π*(C=O)	5.904	0.19
A′	7.343	0.0275	119	19 a′ → 3sσ	7.634	16.61
A″	7.966	0.0047	115	5 a″→ 3sσ		
A″	8.119	0.0001	144	19a′ → 3pπ	8.195	11.91
A′	8.132	0.0407	138	19a′ → 3pσ	8.000	13.26
A′	8.286	0.1359	114	5 a″ → LUMO π*(C=O)	8.394	13.19
A′	8.31	0.0036	160	19a′ → 3pσ′		
A′	8.667	0.0172	197	19a′ → 3dσ	8.372	12.78
A″	8.71	0.0074	146	5a″ → 3pσ		
A′	8.744	0.0098	142	5a″ → 3pπ		
A′	8.856	0.0136	211	19a′ → 3dσ′	8.574	18.95
A″	8.888	0.0039	210	19a′ → 3dπ		
A′	8.92	0.0014	215	19a′ → 3dσ″		
A″	8.923	0.0166	165	5a″ → 3pσ′	9.336	36.68
A″	8.939	0.0033	203	19a′ → 3dπ′		
A′	9.056	0.0102	305	19a′ → 4sσ	8.950	21.66
A″	9.222	<0.0001	401	19a′ → 4pπ	9.171	28.20
A′	9.258	0.0006	421	19a′ → 4pσ	9.090	24.26
A″	9.287	<0.0001	174	5a″ → 3dσ		
A′	9.299	0.0004	449	19a′ → 4pσ′		
A″	9.341	<0.0001	102	18 a′ → LUMO π*(C=O)		
A′	9.424	0.0013	550	19a′ → 4dσ	9.246	31.87
A′	9.503	0.0118	523	19a′ → 4dσ′	9.308	35.47
A″	9.506	0.0019	217	5a″ → 3dσ′		
A″	9.531	0.0006	594	19a′ → 4dπ		
A′	9.534	0.0019	568	19a′ → 4dσ″		
A″	9.536	0.0007	615	19a′ → 4dπ′		
A′	9.543	0.0082	245	5a″ → 3dπ		
A′	9.575	0.0052	359	18a′ → 3sσ		
A″	9.588	<0.0001	214	5a″ → 3dσ″		

at a given altitude corresponds to the local photolysis lifetime. Photolysis lifetimes of less than one year were calculated at altitudes above 22 km. This indicates that ethyl acetate is stable and thus cannot be broken up efficiently by VUV absorption at these altitudes. Even at higher altitudes the lifetimes are of substantial length (e.g. 24 h at 45 km), leading to rather low values of photolysis rates (1.23×10^{-5} s^{-1}), whereas at lower altitudes the lack of solar actinic flux at the absorption wavelengths of this molecule leads to an extremely long lifetime. It is therefore important to assess other possible pathways as a sink mechanisms of this molecule from the atmosphere.

Rate constants for gas-phase reactions of OH, Cl, NO_3 radicals with ethyl acetate have been extensively studied [35–42] and rate constants for reactions at room temperature of $(1.67 \pm 0.22) \times 10^{-12}$, $(1.76 \pm 0.11) \times 10^{-11}$ and $(1.3 \pm 0.3) \times 10^{-17}$, all in cm^3 $molecule^{-1}$ s^{-1}, respectively, were reported. Some studies were also performed on hydroxyl, chlorine, nitrate and sulphate (SO_4^-) radical attack [2] on ethyl acetate in aqueous phase that is of importance for acid rain chemistry. All these cases prove that not only is radical attack the main mechanism for the ester removal from the atmosphere, but also that the order of the reactivities of ethyl acetate with such species would be as follows: Cl ≈ OH ≫ NO_3 ≈ SO_4^-. UV photolysis is not expected to play a significant role in the tropospheric removal of ethyl acetate.

6 Conclusions

We present for the first time the complete electronic spectra of ethyl acetate, together with absolute photoabsorption cross sections from 4.5 to 10.7 eV. The structures observed in the spectrum were assigned to both valence and Rydberg transitions, based on ab initio calculations of vertical excitation energies and oscillator strengths of this molecule. Fine structure has been assigned to vibrational

Table 6. Proposed vibrational assignments in the 6.5−10.0 eV absorption bands of ethyl acetate, $C_4H_8O_2$; t in brackets indicates a tentative assignment.

Energy/eV	Assignment	$\Delta E(\nu'_{28})$/eV	$\Delta E(\nu'_7)$/eV
Second band: π^*(C=O)← n_{O1}(19a′)			
6.986	ν_{00}	–	–
7.045	$1\nu'_7$	–	0.059
7.093	$2\nu'_7$	–	0.048
7.155	$1\nu'_{28}$	0.169	–
7.217	$1\nu'_{28}+1\nu'_7$	–	0.062
7.273	$1\nu'_{28}+2\nu'_7$	–	0.055
7.337	$2\nu'_{28}$	0.182	–
7.394	$2\nu'_{28}+1\nu'_7$	–	0.057
7.441	$2\nu'_{28}+2\nu'_7$	–	0.047
7.496	$3\nu'_{28}$	0.159	–
7.553	$3\nu'_{28}+1\nu'_7$	–	0.057
7.606	$3\nu'_{28}+2\nu'_7$	–	0.053
7.671	$4\nu'_{28}$	0.175	–
7.731	$4\nu'_{28}+1\nu'_7$	–	0.060
7.790(t)	$4\nu'_{28}+2\nu'_7$	–	0.051
7.865	$5\nu'_{28}$	0.194	–
7.923	$5\nu'_{28}+1\nu'_7$	–	0.058
7.978	$5\nu'_{28}+2\nu'_7$	–	0.055
8.029	$6\nu'_{28}$	0.164	–
8.076	$6\nu'_{28}+1\nu'_7$	–	0.047
8.121	$6\nu'_{28}+2\nu'_7$	–	0.045
Fourth band: 3sσ ←(19a′)			
8.155	ν_{00}	–	–
8.212	$1\nu'_7$	–	0.057
8.267	$2\nu'_7$	–	0.055
High energy region: 9.0−10.0 eV			
9.125	ν_{00}	–	–
9.177	$1\nu'_7$	–	0.052
9.299	$1\nu'_{28}$	0.174	–
9.350	$1\nu'_{28}+1\nu'_7$	–	0.051
9.486	$2\nu'_{28}$	0.187	–
9.537	$2\nu'_{28}+1\nu'_7$	–	0.051

series involving predominantly excitations of ν_{28} and ν_7 modes that are due to C−O and C=O stretches and OCC deformation combined with CO stretch and CH_3 rocking, respectively. In the He(I) photoelectron spectrum of ethyl acetate, vibrational excitations in the first ionic state were resolved and also assigned to ν_{28} and ν_7 modes. The theoretical calculations presented here are in a good agreement with experimental data. Based on the photoabsorption cross section, photolysis lifetimes of ethyl acetate have been calculated for the Earth's troposphere and stratosphere and based on the literature values of rate constants for the reactions of ethyl acetate with hydroxyl, chlorine, nitrate and sulphate radicals, photolysis was excluded as a significant process of removal of this compound from the atmosphere.

M.A.Ś. acknowledges the visiting fellow position in the Molecular Physics Group, Open University. P.L.V. acknowledges the Portuguese National Funding Agency (FCT-MCTES) through grants PTDC/FIS-ATO/1832/2012 and UID/FIS/00068/2013. The authors wish to acknowledge the beam time at the ASTRID synchrotron at Aarhus University, Denmark, supported by the European Union (EU) I3 programme ELISA, Grant Agreement No. 226716. We also acknowledge the financial support provided by the European Commission through the Access to Research Infrastructure action of the Improving Human Potential Programme. J.G. and M.Ł. are thankful to the 7th Framework Programme of the European Union (grant agreement No. 321971). All calculations have been performed at the Academic Center (CI TASK) in Gdańsk and at Universitätsrechenzentrum of the Friedrich-Schiller University in Jena.

References

1. I. Medvedev, F.C.D. Lucia, E. Herbst, A&A **499**, 215 (2009)
2. G.V. Buxton, J. Wang, G.A. Salmon, Phys. Chem. Chem. Phys. **3**, 2618 (2001)
3. D. Helmig, J. Möller, W. Klein, Chemosphere **19**, 1399 (1989)
4. J.D. Morrison, A.J.C. Nicholson, J. Chem. Phys. **20**, 1021 (1952)
5. A.G. Harrison, A. Ivko, D. van Raalte, Can. J. Chem. **44**, 1625 (1966)
6. J.L. Holmes, F.P. Lossing, J. Am. Chem. Soc. **102**, 1591 (1980)
7. K. Watanabe, J. Chem. Phys. **26**, 542 (1957)
8. D.A. Sweigart, D.W. Turner, J. Am. Chem. Soc. **94**, 5592 (1972)
9. F.M. Benoit, A.G. Harrison, J. Am. Chem. Soc. **99**, 3980 (1977)
10. L. Fraser-Monteiro, M.L. Fraser-Monteiro, J.J. Butler, T. Baer, J. Phys. Chem. **86**, 752 (1982)
11. Y. Nunes, G. Martins, N.J. Mason, D. Duflot, S.V. Hoffmann, J. Delwiche, M.J. Hubin-Franskin, P. Limão-Vieira, Phys. Chem. Chem. Phys. **12**, 15734 (2010)
12. M.A. Śmiałek, M. Łabuda, J. Guthmuller, M.J. Hubin-Franskin, J. Delwiche, D. Duflot, N.J. Mason, S.V. Hoffmann, N.C. Jones, P. Limão-Vieira, J. Chem. Phys. **141**, 104311 (2014)
13. M.A. Śmiałek, M. Łabuda, J. Guthmuller, S.V. Hoffmann, N.C. Jones, M.A. MacDonald, L. Zuin, N.J. Mason, P. Limão-Vieira, J. Phys. Chem. A **119**, 8647 (2015)
14. T. Ha, C. Pal, P.N. Ghosh, Spectrochim. Acta A **48**, 1083 (1992)
15. S. Eden, P. Limão-Vieira, S. Hoffmann, N. Mason, Chem. Phys. **323**, 313 (2006)
16. N. Mason, J. Gingell, J. Davies, H. Zhao, I. Walker, M. Siggel, J. Phys. B **29**, 3075 (1996)
17. W.F. Chan, G. Cooper, C.E. Brion, Phys. Rev. A **44**, 186 (1991)
18. J. Delwiche, P. Natalis, J. Momigny, J.E. Collin, J. Electron Spectrosc. Relat. Phenom. **1**, 219 (1972-1973)
19. K.P. Huber, C. Jungen, J. Chem. Phys. **92**, 850 (1990)
20. D.A. Shaw, D.M.P. Holland, M.A. MacDonald, A. Hopkirk, M.A. Hayes, S.M. McSweeney, Chem. Phys. **166**, 379 (1992)
21. P.H. van Cittert, Z. Phys. **69**, 298 (1931)

22. K.A.G. Macneil, R. Dixon, J. Electron Spectrosc. Relat. Phenom. **11**, 315 (1977)
23. M.J. Hubin-Franskin, J. Delwiche, P. Natalis, G. Caprace, D. Roy, J. Electron Spectrosc. Relat. Phenom. **18**, 295 (1980)
24. P.T. Ruhoff, Chem. Phys. **186**, 355 (1994)
25. M. Łabuda, J. Guthmuller, Eur. Phys. J. Special Topics **222**, 2257 (2013)
26. J. Guthmuller, F. Zutterman, B. Champagne, J. Chem. Theor. Comput. **4**, 2094 (2008)
27. J. Guthmuller, F. Zutterman, B. Champagne, J. Chem. Phys. **131**, 154302 (2009)
28. K. Kaufmann, W. Baumeister, M. Jungen, J. Phys. B **22**, 2223 (1989)
29. H.J. Werner, P.J. Knowles, G. Knizia, F.R. Manby, M. Schütz, P. Celani, T. Korona, R. Lindh, A. Mitrushenkov, G. Rauhut, K.R. Shamasundar, T.B. Adler, R.D. Amos, A. Bernhardsson, A. Berning, D.L. Cooper, M.J.O. Deegan, A.J. Dobbyn, F. Eckert, E. Goll, C. Hampel, A. Hesselmann, G. Hetzer, T. Hrenar, G. Jansen, C. Köppl, Y. Liu, A.W. Lloyd, R.A. Mata, A.J. May, S.J. McNicholas, W. Meyer, M.E. Mura, A. Nicklass, D.P. O'Neill, P. Palmieri, D. Peng, K. Pflüger, R. Pitzer, M. Reiher, T. Shiozaki, H. Stoll, A.J. Stone, R. Tarroni, T. Thorsteinsson, M. Wang, Molpro, version 2012.1, a package of ab initio programs (2012), http://www.molpro.net
30. P. Sinha, S.E. Boesch, C. Gu, R.A. Wheeler, A.K. Wilson, J. Phys. Chem. A **108**, 9213 (2004)
31. J.E. Saunders, J.J. Lucier, F.F. Bentley, Appl. Spectrosc. **22**, 697 (1968)
32. M. Oki, H. Nakanishi, Bull. Chem. Soc. Jpn **43**, 2558 (1970)
33. W.B. DeMore, S.P. Sander, D.M. Golden, R.F. Hampson, M.J. Kurylo, C.J. Howard, A.R. Ravishankara, C.E. Kolb, M.J. Molina, Chemical kinetics and photochemical data for use in stratospheric modeling, Evaluation Number 12, January 15, JPL Publication 97-4, 1997
34. P. Limão-Vieira, S. Eden, P. Kendall, N. Mason, S. Hoffmann, Chem. Phys. Lett. **364**, 535 (2002)
35. T.J. Wallington, P. Dagaut, R. Liu, M.J. Kurylo, Int. J. Chem. Kinet. **20**, 177 (1988)
36. A.E. Boudali, S.L. Calvé, G.L. Bras, A. Mellouki, J. Phys. Chem. **100**, 12364 (1996)
37. I.M. Campbell, P.E. Parkinson, Chem. Phys. Lett. **53**, 385 (1978)
38. J.J. Orlando, G.S. Tyndall, Int. J. Chem. Kinet. **42**, 397 (2010)
39. C.A. Cuevas, A. Notario, E. Martínez, J. Albaladejo, Atmospheric Environment **39**, 5091 (2005)
40. A. Notario, G.L. Bras, A. Mellouki, J. Phys. Chem. A **102**, 3112 (1998)
41. J.H. Xing, K. Takahashi, M.D. Hurley, T.J. Wallington, Chem. Phys. Lett. **474**, 268 (2009)
42. S. Langer, E. Ljungström, I. Wängberg, J. Chem. Soc., Faraday Trans. **89**, 425 (1993)
43. M.J. Frisch et al., *Gaussian 09, revision A.02* (Gaussian Inc., Wallingford, CT, 2009)